The Complete Treatise on Detecting Radioactive Particles and Radiation

Soumadeep Ghosh

Kolkata, India

Abstract

This comprehensive treatise provides a thorough examination of radioactive particle and radiation detection, encompassing theoretical foundations from nuclear physics, detection principles, instrumentation technologies, applications across diverse fields, safety considerations, calibration methodologies, and emerging research developments. The work synthesizes knowledge from nuclear physics, materials science, electronics engineering, and applied radiation measurements to present the current state-of-the-art in radiation detection technologies and methodologies. Key areas covered include fundamental nuclear processes, detection mechanisms, instrument design principles, performance characteristics, calibration procedures, safety protocols, and future technological developments including quantum sensors, artificial intelligence applications, and advanced materials.

The treatise ends with "The End"

Contents

List of Figures

1 Introduction

The detection and measurement of ionizing radiation represents one of the most critical technological capabilities in modern society, with applications spanning medical diagnostics and treatment, nuclear power generation, environmental monitoring, homeland security, and fundamental scientific research. This comprehensive treatise examines the theoretical foundations, technological implementations, practical applications, and future developments in radiation detection systems.

The field has evolved dramatically since the early discoveries of radioactivity by Becquerel, the Curies, and Rutherford. From simple electroscopes and photographic plates, detection technology has advanced to sophisticated digital spectrometry systems capable of real-time isotope identification, wireless networking, and artificial intelligence-enhanced analysis. Modern detection systems achieve energy resolutions below 0.1 %, count rates exceeding 1×10^6 cps, and sensitivities approaching individual particle detection.

This work addresses the complete spectrum of radiation detection knowledge, from the fundamental nuclear physics governing radioactive decay to the cutting-edge quantum sensors and machine learning algorithms that represent the future of the field. The systematic approach begins with theoretical foundations, progresses through technological implementations, examines practical applications, and concludes with emerging research directions.

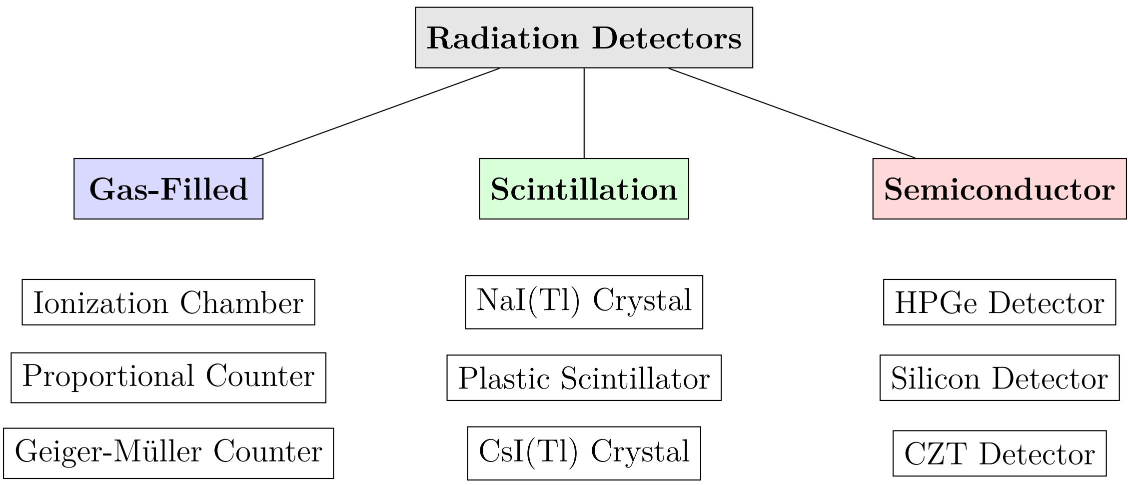

Figure 1: Classification of radiation detector types arranged in vertical hierarchy

2 Theoretical Foundations from Nuclear Physics and Chemistry

2.1 Nuclear Structure and Stability

The fundamental understanding of radiation detection begins with nuclear physics principles governing atomic nuclei stability and radioactive decay. Nuclear binding energy, described by the semi-empirical mass formula, determines nuclear stability through the competition between the strong nuclear force providing binding and electromagnetic repulsion between protons.

The nuclear shell model explains nuclear structure through magic numbers (2, 8, 20, 28, 50, 82, 126), while the liquid drop model describes collective nuclear behavior. Nuclei with proton numbers Z > 82 are inherently unstable due to Coulomb repulsion, leading to spontaneous decay processes that produce detectable radiation.

Nuclear stability criteria depend on the neutron-to-proton ratio (N/Z). Excess neutrons lead to β^- decay, excess protons result in β^+ decay or electron capture, and heavy nuclei undergo α decay or spontaneous fission. The nuclear binding energy per nucleon curve, peaking around ^{56}Fe, explains the energy release in both fusion and fission processes.

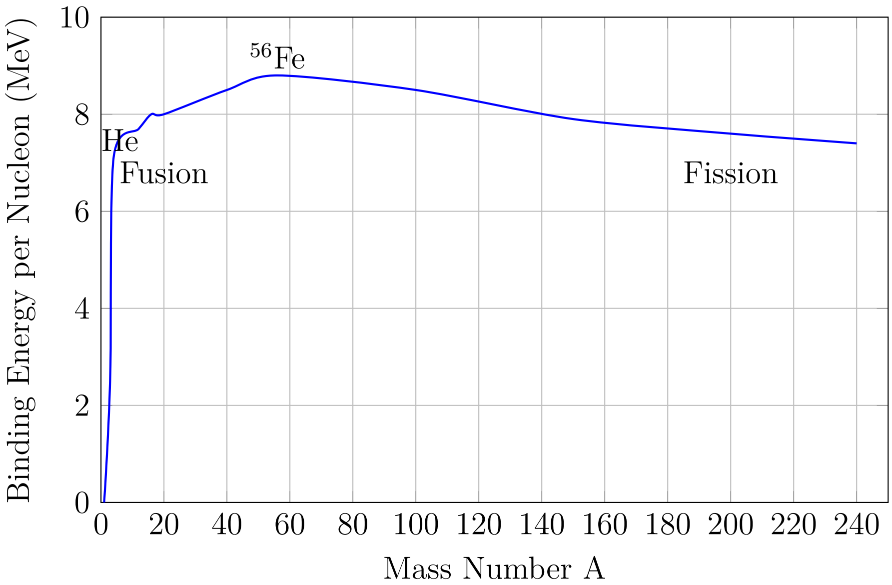

Figure 2: Nuclear binding energy per nucleon versus mass number showing regions where fusion and fission release energy

2.2 Radioactive Decay Processes

2.2.1 Fundamental Decay Law

The exponential decay law governs all radioactive processes:

$$N(t) = N_0 e^{-\lambda t} \tag{1}$$

where $N(t)$ represents the number of radioactive nuclei at time t, N_0 is the initial number, and λ is the decay constant. The relationship between decay constant and half-life is:

$$t_{1/2} = \frac{\ln(2)}{\lambda} = \frac{0.693}{\lambda} \tag{2}$$

Activity, representing the decay rate, follows:

$$A(t) = \lambda N(t) = A_0 e^{-\lambda t} \tag{3}$$

Activity units include the Becquerel (Bq), defined as one decay per second (SI unit), and the Curie (Ci), equal to 3.7×10^{10} Bq (historically based on ^{226}Ra activity).

2.2.2 Decay Chain Mathematics

For sequential decay processes A $\rightarrow$ B $\rightarrow$ C, the daughter nucleus activity evolution follows:

$$N_B(t) = \frac{\lambda_A N_{0A}}{\lambda_B - \lambda_A}(e^{-\lambda_A t} - e^{-\lambda_B t}) \tag{4}$$

Secular equilibrium occurs when $\lambda_A \ll \lambda_B$, yielding $\lambda_A N_A = \lambda_B N_B$. This condition is important in natural decay series and explains the equilibrium between radon and its short-lived progeny in environmental monitoring.

2.3 Types of Radioactive Particles and Radiation

2.3.1 Alpha Particles

Alpha particles are helium-4 nuclei ($^4He^{2+}$) typically carrying 4-9 MeV kinetic energy. The decay process follows:

$$^A_Z X \rightarrow ^{A-4}_{Z-2} Y + ^4_2 He^{2+} \tag{5}$$

Alpha particles exhibit high ionization density (approximately 100 ion pairs per micrometer in air), short range (few centimeters in air), and are stopped by thin materials (paper, dead skin layer). Detection requires thin-window detectors or windowless configurations for direct measurement.

2.3.2 Beta Particles

Beta decay involves weak nuclear force interactions. β^- decay converts neutrons to protons:

$$^A_Z X \rightarrow ^A_{Z+1} Y + e^- + \overline{\nu_e} \tag{6}$$

β^+ decay (positron emission) converts protons to neutrons:

$$^A_Z X \rightarrow ^A_{Z-1} Y + e^+ + \nu_e \tag{7}$$

Beta particles exhibit continuous energy spectra from zero to the Q-value (endpoint energy), with mean energy approximately one-third of the maximum energy. The neutrino carries away variable energy, creating the characteristic continuous spectrum.

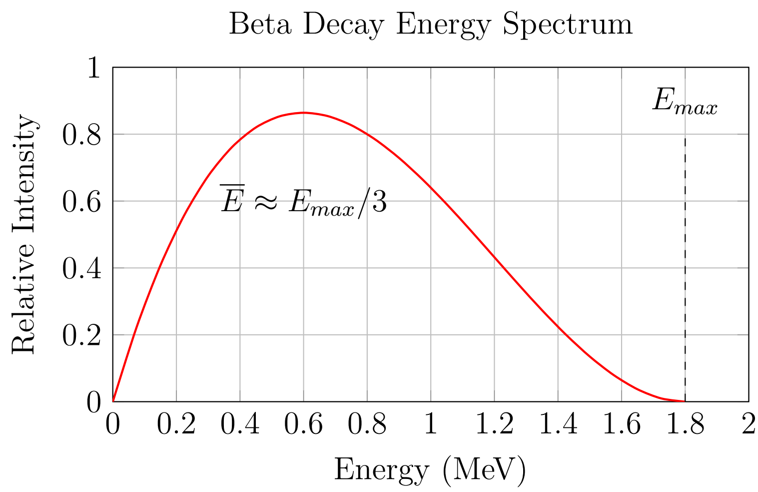

Figure 3: Beta particle energy spectrum showing continuous distribution with maximum energy E_{max}

2.3.3 Gamma Rays

Gamma rays are high-energy electromagnetic radiation (photons) with no mass or charge. They represent nuclear transitions between excited and ground states, often following alpha or beta decay. Gamma energies are characteristic of specific nuclear transitions, providing isotope identification capability through spectroscopy.

2.3.4 Neutrons

Neutrons present unique detection challenges due to their electrical neutrality. Detection requires nuclear reactions producing charged particles:

$$^{3}He + n \rightarrow ^{3} H + ^{1} H + 764 \text{ keV} \tag{8}$$

$$^{10}B + n \rightarrow ^{7} Li + \alpha + 2.31 \text{ MeV} \tag{9}$$

Neutron energy categories include thermal (0.025 eV), epithermal (1 eV - 1 keV), and fast (>1 keV), each requiring different detection approaches.

2.4 Radiation Interaction Mechanisms with Matter

Understanding radiation-matter interactions is fundamental to detector design and performance optimization.

2.4.1 Photon Interactions

Photoelectric Effect: Complete photon absorption by inner shell electrons with probability $\tau \propto Z^{4-5}/E^3$. The photoelectron kinetic energy equals $E_{\text{photoelectron}} = h\nu - E_{\text{binding}}$.

Compton Scattering: Inelastic scattering with atomic electrons. The scattered photon energy follows:

$$h\nu' = \frac{h\nu}{1 + \alpha(1 - \cos\theta)} \tag{10}$$

where $\alpha = h\nu/(m_e c^2)$ and θ is the scattering angle.

Pair Production: Creation of electron-positron pairs with threshold energy $h\nu \geq$ 1.022 MeV. The kinetic energies satisfy $E_{e^+} + E_{e^-} = h\nu - 1.022$ MeV.

The total linear attenuation coefficient combines all processes: $\mu = \tau + \sigma + \kappa$, leading to Beer-Lambert law attenuation: $I = I_0 e^{-\mu x}$.

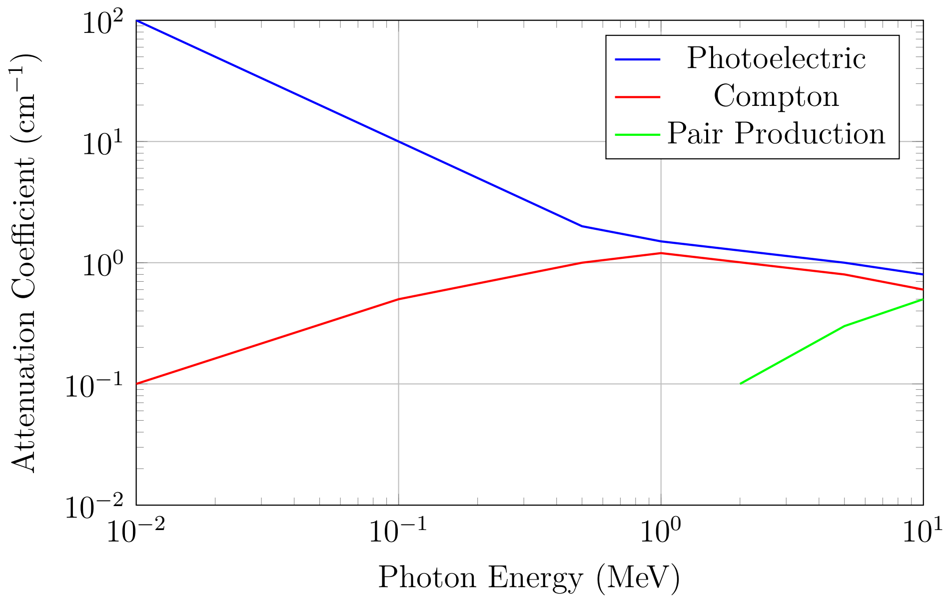

Figure 4: Photon attenuation mechanisms in lead as a function of energy

2.4.2 Charged Particle Interactions

Charged particles lose energy continuously through electromagnetic interactions described by the Bethe-Bloch formula. Energy loss exhibits the characteristic Bragg peak behavior, with maximum energy deposition near the end of the particle range.

3 Detection Principles and Mechanisms

3.1 Fundamental Detection Mechanisms

Radiation detection relies on energy transfer from incident radiation to detector material, creating measurable signals through ionization, excitation, or heat generation.

3.1.1 Ionization Process

When ionizing radiation interacts with detector material, it removes orbital electrons from atoms, creating ion pairs. The W-value represents the mean energy expended per charge carrier pair:

$$N = \frac{E}{W} \tag{11}$$

where N is the number of charge carriers produced and E is the deposited energy. W-values are approximately 30-35 eV per ion pair in gases and 3.6 eV per electron-hole pair in silicon.

3.1.2 Signal Formation

The Shockley-Ramo theorem describes current induction by moving charges:

$$i(t) = q \cdot v(t) \cdot E_w(x) \tag{12}$$

where q is the charge, $v(t)$ is the instantaneous velocity, and $E_w(x)$ is the weighting field at position x. Charge-sensitive preamplifiers convert collected charge to proportional voltage: $V_{\text{out}} = Q/C_f$.

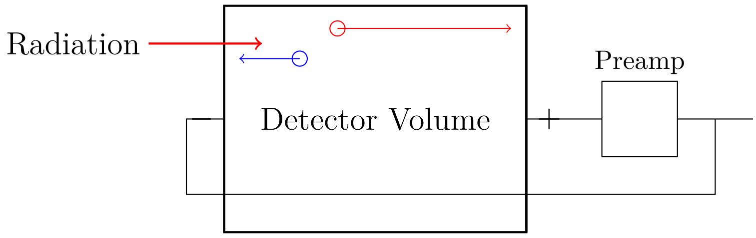

Basic Detector Principle

Figure 5: Fundamental radiation detection mechanism showing charge collection and signal processing

3.2 Gas-Filled Detectors

3.2.1 Ionization Chambers

Ionization chambers operate in the ion saturation region without gas amplification. Current mode operation yields:

$$I = \frac{dN}{dt} \times W \times e \tag{13}$$

where I is the current, dN/dt is the interaction rate, W is the W-value, and e is the elementary charge.

3.2.2 Proportional Counters

Gas multiplication occurs through Townsend avalanche when electric fields exceed approximately 10^4 V/cm. The multiplication factor follows:

$$M = \exp\left(\int \alpha \, dx\right) \tag{14}$$

where α is the first Townsend coefficient related to gas pressure and field strength by $\alpha/p = A \exp(-Bp/E)$.

3.2.3 Geiger-Müller Counters

Geiger counters operate in the avalanche breakdown region, producing output pulses of identical amplitude regardless of initial radiation energy. Dead time limitations restrict count rates to approximately 10^4 cps maximum.

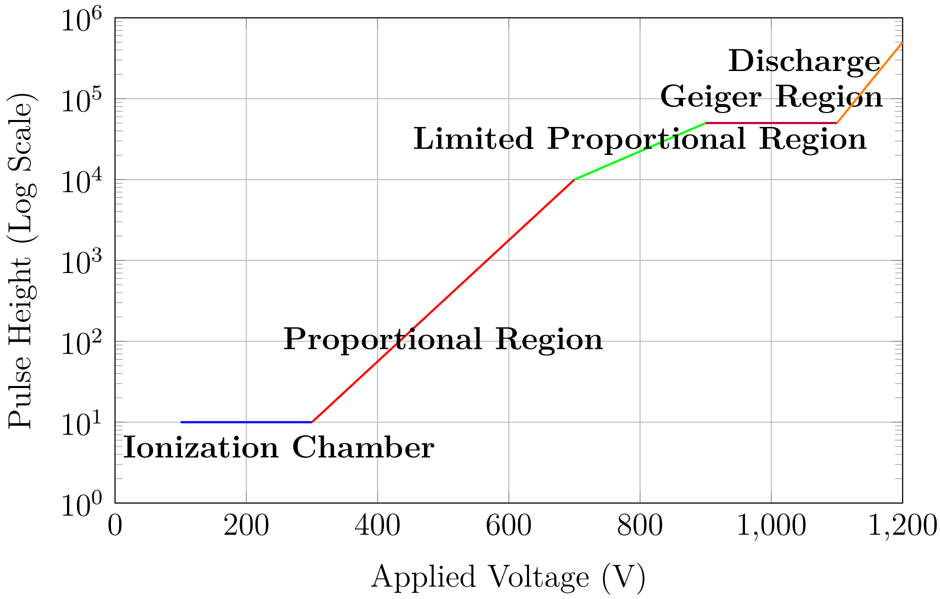

Figure 6: Gas amplification regions showing different detector operating modes

3.3 Scintillation Detection

3.3.1 Scintillation Mechanisms

Scintillation involves three stages: conversion (radiation to electron-hole pairs), energy transfer (migration to luminescent centers), and luminescence (radiative recombination). Scintillation efficiency follows:

$$\eta = \gamma S Q \tag{15}$$

where γ is conversion efficiency, S is energy transfer efficiency, and Q is quantum efficiency of luminescent centers.

3.3.2 Scintillator Materials

Inorganic Scintillators: NaI(Tl) provides high light yield (41,000 photons/MeV) with 230 ns decay time. CsI(Tl) offers lower hygroscopicity for harsh environments. Modern materials like Lu_2SiO_5:Ce (LSO) combine high light yield (30,000 photons/MeV) with fast timing (40 ns decay).

Organic Scintillators: Based on π-electron transitions, these materials provide fast response (nanosecond scale) suitable for neutron detection through proton recoil.

3.3.3 Photodetectors

Photomultiplier Tubes (PMTs): Convert scintillation light to electrical signals with gains of 10^6–10^8. Quantum efficiency reaches 25–43% for bialkali photocathodes.

Silicon Photomultipliers (SiPMs): Arrays of avalanche photodiodes in Geiger mode offer low voltage operation (30–70V), magnetic field insensitivity, and high photon detection efficiency (>50%).

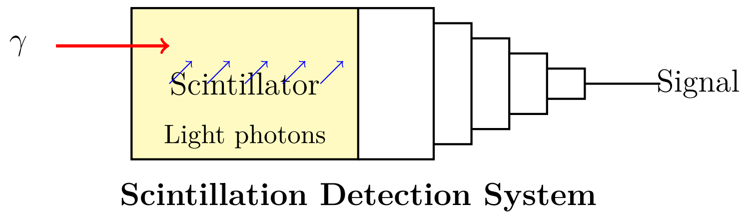

Figure 7: Scintillation detector components showing light production and photodetection

3.4 Semiconductor Detectors

3.4.1 Charge Collection Physics

Semiconductor detectors utilize reverse-biased p-i-n structures creating depletion regions. Depletion depth follows:

$$d = \sqrt{\frac{2\varepsilon V_{\text{bias}}}{eN_{\text{eff}}}} \tag{16}$$

where ε is permittivity, V_{bias} is applied voltage, and N_{eff} is effective doping concentration.

3.4.2 Energy Resolution

Energy resolution depends on statistical fluctuations, electronic noise, and charge collection variations:

$$\Delta E^2 = \Delta E_1^2 + \Delta E_2^2 + \Delta E_3^2 \tag{17}$$

Statistical limitations follow: $\Delta E_1 \propto \sqrt{FE}$ where F is the Fano factor.

3.5 Performance Parameters

3.5.1 Detection Efficiency

Total efficiency combines geometric and intrinsic components:

$$\varepsilon_{\text{total}} = \varepsilon_{\text{geometric}} \times \varepsilon_{\text{intrinsic}} \tag{18}$$

Geometric efficiency for point sources: $\varepsilon_{\text{geom}} = \Omega/(4\pi) = (1/2)[1 - d/\sqrt{d^2 + R^2}]$

3.5.2 Dead Time

Two models describe dead time behavior:

- **Non-paralyzable**: $m = n/(1 + n\tau)$
- **Paralyzable**: $m = n\exp(-n\tau)$

where m is observed count rate, n is true count rate, and τ is dead time.

4 Comprehensive Overview of Detection Instruments and Technologies

4.1 High-Purity Germanium (HPGe) Detectors

HPGe detectors achieve superior energy resolution through low W-value (2.96 eV per electron-hole pair) and minimal statistical fluctuations. Performance specifications include energy resolution less than 2 keV FWHM at 1.33 MeV, peak-to-Compton ratio greater than 50:1 for 1.33 MeV, relative efficiency up to 200% compared to 3 inch by 3 inch NaI(Tl), and operating temperature of 77K requiring liquid nitrogen cooling.

Design types include coaxial detectors with n-type or p-type central contact configurations, planar detectors optimized for low-energy photon detection, well-type detectors with enhanced efficiency for small samples, and segmented detectors providing position sensitivity and Compton suppression.

4.2 Neutron Detection Systems

The helium-3 shortage since 2008 has driven development of alternative neutron detection technologies. Helium-3 detectors utilize the nuclear reaction ^{3}He + n $\rightarrow$ ^{3}H + ^{1}H + 764 keV, which provides high cross section (5,330 barns) for thermal neutrons with excellent gamma discrimination. Supply limitations have increased costs dramatically and driven alternative technology development.

Boron-based detectors employ boron trifluoride (BF_3) through the reaction ^{10}B + n $\rightarrow$ ^{7}Li + α + 2.31 MeV (94% branch) providing neutron detection with 3,840 barn cross section. Toxic and corrosive gas properties require careful handling. Boron-lined detectors use ^{10}B or $^{10}B_4C$ coatings (0.2–0.5 mg/cm^2) on tube walls with non-toxic P-10 fill gas. Lower sensitivity (approximately 4 cps/nv) compared to ^{3}He but similar gamma rejection capabilities.

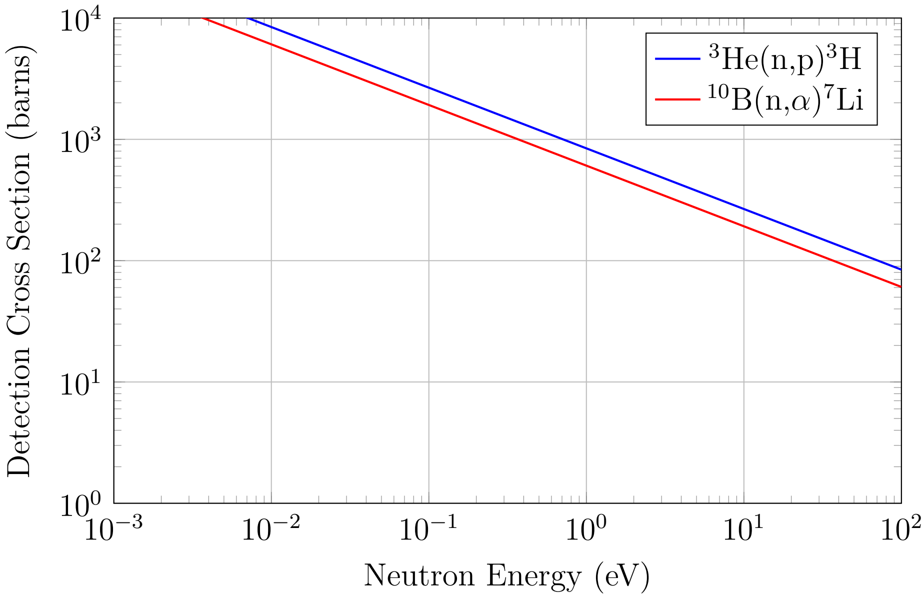

Figure 8: Neutron detection cross sections for thermal neutron reactions showing the characteristic $1/v$ dependence for thermal neutrons

4.3 Personal Dosimetry

4.3.1 Thermoluminescent Dosimeters (TLD)

TLD materials store radiation energy in crystal lattice traps, releasing it as light upon heating to approximately 300 degrees Celsius. Common materials include LiF:Mg,Ti (TLD-100) which is tissue equivalent with dose range 10 μGy to 10 Gy, CaF_2:Dy (TLD-200) with high sensitivity for environmental monitoring, and LiF:Mg,Cu,P (TLD-100H) with enhanced sensitivity for low-dose applications.

Performance characteristics include less than 5% fading in 3 months and reusability for greater than 1000 cycles.

4.3.2 Optically Stimulated Luminescence (OSL)

Al_2O_3:C is the standard OSL material, offering re-readability through non-destructive readout, faster processing, and better fade characteristics compared to TLD systems. Green LED stimulation (525 nm) produces blue light emission (420 nm) proportional to radiation dose.

4.3.3 Electronic Personal Dosimeters (EPD)

Real-time dose measurement using silicon diode detectors, GM detectors, MOSFET devices, or scintillator-photodiode combinations. Features include digital displays, alarm capabilities, data logging, wireless communication, and GPS location tracking.

4.4 Portal Monitors and Large-Area Detection Systems

4.4.1 Radiation Portal Monitors (RPM)

RPM systems screen vehicles and cargo at border crossings, ports, and nuclear facilities. System architecture includes gamma detection using plastic scintillator (PVT) or NaI(Tl) arrays for general radiation detection, neutron detection using ^{3}He tubes (being replaced) or boron-lined detectors for special nuclear material detection, electronics with multichannel analyzers and digital signal processing, and mechanical pillar design typically 4–6 meters wide accommodating vehicle traffic.

Performance requirements per ANSI N42.35 standards include specified detection sensitivities, false alarm rates less than 1 in 10,000 passages, and environmental operation from -40 degrees Celsius to +70 degrees Celsius.

4.4.2 Advanced Spectroscopic Portals (ASP)

Second and third-generation systems incorporate NaI(Tl) arrays or high-resolution CZT detectors for isotope identification capability. Challenges include high cost versus performance benefits, maintenance requirements for cooled systems, and nuisance alarms from naturally occurring radioactive materials (NORM).

4.5 Digital Signal Processing and Modern Electronics

4.5.1 Digital Multichannel Analyzers

Modern systems employ full digital processing with FPGA-based real-time algorithms. Key components include 12–16 bit ADCs with 50–500 MHz sampling rates, FPGA processors for real-time pulse analysis, DSP algorithms for complex spectral processing, and multi-event buffering with list mode data acquisition.

Advantages include flexibility, stability, and advanced algorithms including pile-up rejection, baseline restoration, and digital filtering that optimize detector performance.

4.5.2 Advanced Signal Processing

Digital pulse processing employs trapezoidal shaping, maximum likelihood estimation for timing, and pulse shape discrimination for particle identification. Machine learning integration utilizes neural networks for isotope identification, anomaly detection algorithms, and real-time spectral analysis achieving greater than 93% accuracy in radioisotope identification.

5 Modern Detection Methods and Emerging Technologies

5.1 Digital Revolution in Radiation Detection

The transition from analog to fully digital processing has transformed radiation detection capabilities. Modern systems achieve superior performance through real-time processing using FPGA-based systems with 14-bit resolution and 125 MHz sampling enabling simultaneous processing of up to 64 detector channels.

Advanced algorithms include digital filtering techniques (CR-RC, trapezoidal shaping), pulse shape discrimination, and adaptive baseline restoration that optimize detector performance beyond analog limitations. Flexibility through reconfigurable digital systems allows adaptation to different detector types and measurement requirements without hardware changes.

5.2 Artificial Intelligence and Machine Learning Applications

AI integration represents a paradigm shift in radiation detection analysis.

5.2.1 Pattern Recognition Systems

Convolutional Neural Networks (CNNs) achieve greater than 93% accuracy in gamma-ray spectroscopy, outperforming traditional peak-fitting algorithms by 2–12%. Automated isotope identification using neural networks trained on comprehensive spectral libraries enables real-time radioisotope identification with 98.63% accuracy for 14 target radionuclides. Anomaly detection through machine learning algorithms detects unusual radiation events in real-time, enabling rapid response to potential threats.

5.2.2 Explainable AI (XAI)

Recent developments in interpretable machine learning using SHAP (SHapley Additive exPlanations) and LIME (Local Interpretable Model-agnostic Explanations) provide transparency in AI-driven spectral analysis decisions.

5.3 Quantum Sensing Technologies

5.3.1 Nitrogen-Vacancy Centers

Diamond-based NV centers enable detection of individual nuclear quadrupolar resonance signals at room temperature, achieving unprecedented molecular-level sensitivity.

5.3.2 Superconducting Quantum Detectors

Thermal Kinetic Inductance Detectors (TKIDs) achieve tens of eV energy resolution for X-ray and gamma-ray spectroscopy with single-photon sensitivity. These systems operate at sub-1K temperatures and enable kilo-pixel arrays for large-area detection.

5.4 Advanced Materials Development

5.4.1 Perovskite Semiconductors

$CsPbBr_3$ represents the most significant breakthrough in detector materials, demonstrating energy resolutions of 2.5% at 141 keV and 1.0% at 662 keV, solution-based processing for cost-effective manufacturing, superior stopping power compared to traditional CZT detectors, and self-healing capabilities with radiation tolerance.

5.4.2 Nanostructured Scintillators

Photonic crystal coatings provide up to 6-fold enhancement in light yield through nanostructured surfaces. Meta-scintillators combine high-Z stopping materials with fast emitters for improved timing resolution. Flexible nanocomposites enable conformable detectors for imaging non-flat objects in medical applications.

5.5 Wireless and Distributed Detection Networks

5.5.1 MEMS-Based Sensors

Microelectromechanical systems enable autonomous wireless sensor nodes with volumes ranging from cubic millimeters to cubic centimeters, incorporating energy harvesting capabilities for long-term deployment in distributed radiation monitoring networks.

5.5.2 IoT Integration

Internet of Things platforms enable smart monitoring systems with edge computing, local data processing, and machine learning algorithms for automated alerting and anomaly detection.

6 Applications in Various Fields

6.1 Medical Applications

6.1.1 Nuclear Medicine and Medical Imaging

Modern positron emission tomography and single photon emission computed tomography systems utilize advanced detector materials achieving improved performance. Timing resolution in current systems achieves 214–380 ps with research targeting 10 ps for time-of-flight PET. Spatial resolution reaches 0.4–0.6 mm in preclinical systems using pixelated detectors. Energy resolution has improved from 10% (BGO) to less than 3% with modern scintillators.

Total-body PET systems with extended axial field-of-view (106–194 cm) provide 40 times sensitivity increase for total-body imaging and 3–4 times improvement for organ-specific studies, enabling reduced radiation doses and faster acquisition times.

Advanced scintillators such as $CeBr_3$ (66,000 photons/MeV) improve energy resolution from 8% to 4%, while GAGG achieves 5% energy resolution with 58,000 photons/MeV light output.

6.1.2 Radiotherapy Monitoring

Comprehensive dosimetry systems ensure patient safety and treatment accuracy through thermoluminescent dosimeters (TLDs) providing high accuracy, reusable systems for patient and occupational monitoring, electronic personal dosimeters (EPDs) for real-time monitoring with digital readouts and alarm capabilities, and ionization chambers for precision calibration of radiological equipment and dose rate monitoring.

6.2 Nuclear Power Industry

6.2.1 Reactor Monitoring and Control

Nuclear power facilities require sophisticated radiation monitoring systems. In-core neutron detection monitors reactor power distribution and flux profiles using fission chambers and neutron-sensitive detectors operating in extreme radiation and temperature environments. Area radiation monitoring provides continuous surveillance of work environments using fixed and portable detection systems meeting regulatory requirements for worker protection. Effluent monitoring of stack and liquid discharge uses gas-flow proportional counters and liquid scintillation systems to ensure environmental compliance.

6.2.2 Waste Management and Characterization

Segmented gamma scanning provides non-destructive assay of waste drums using collimated HPGe detectors for isotopic identification and activity quantification. Neutron assay employs passive neutron counting systems for plutonium detection and characterization in transuranic waste streams. Alpha spectroscopy enables high-resolution analysis for transuranic waste classification and disposal pathway determination.

6.3 Environmental Monitoring

6.3.1 Comprehensive Monitoring Networks

The IAEA International Radiation Monitoring Information System (IRMIS) represents the global standard with 48 participating countries operating greater than 6,000 monitoring stations worldwide providing real-time data for emergency response.

Detection technologies include alpha/beta continuous air monitors with dual-detector systems for particulate monitoring, noble gas monitors using beta-gamma coincidence detection for xenon and krypton isotopes, and tritium-in-air monitors employing liquid scintillation-based systems for low-energy beta detection.

6.3.2 Environmental Assessment Capabilities

Gamma spectroscopy using HPGe detectors provides isotopic analysis for soil, water, and vegetation samples with detection limits in the mBq range. Liquid scintillation is essential for low-energy beta emitters (^{3}H, ^{14}C, ^{63}Ni) in environmental matrices. Radon detection employs track-etch detectors for long-term passive measurement and continuous monitors for real-time assessment.

6.4 Security and Homeland Security Applications

6.4.1 Border Control Systems

The U.S. Customs and Border Protection operates greater than 1,300 Radiation Portal Monitors scanning 100% of containerized cargo and personal vehicles entering the country.

Performance improvements include Revised Operational Settings (ROS) developed by PNNL for optimization reducing nuisance alarms while maintaining threat detection sensitivity, spectroscopic capabilities using energy-based algorithms for NORM discrimination, and mobile systems with 60 mobile RPMs for flexible deployment.

6.4.2 Nuclear Materials Detection

Advanced detection systems employ passive/active interrogation combining detection modalities for enhanced special nuclear material sensitivity, neutron detection using alternative technologies replacing ^{3}He for concealed fissile material detection, and multi-modal screening integrating X-ray/gamma imaging with neutron interrogation.

6.4.3 Handheld and Portable Systems

Radioisotope Identification Devices (RIIDs) use CZT-based systems achieving room-temperature gamma spectroscopy with libraries exceeding 37 isotopes per ANSI N42.34 standards. Personal Radiation Detectors (PRDs) are belt-worn devices for frontline officers with sensitivity thresholds less than 10 nSv/h above background and greater than 1000 hour battery life.

6.5 Research Applications

6.5.1 High-Energy Physics

The Large Hadron Collider employs greater than 400 radiation monitoring devices for electronics protection, with requirements for radiation tolerance to 1 MGy doses in HL-LHC environments.

Advanced detector technologies include Low Gain Avalanche Detectors (LGADs) with built-in gain and fast readout for timing applications, silicon pixel detectors with 10 micrometer spatial resolution for particle tracking, and calorimeter systems for electromagnetic and hadronic energy measurement.

6.5.2 Space Applications

Radiation environment monitoring employs multi-detector telescopes for cosmic ray flux measurement, real-time monitoring for crew protection during solar particle events, and neutron spectrometry for energy spectrum analysis.

Space-qualified systems such as the Hybrid Electronic Radiation Assessor (HERA) demonstrate Timepix-based detection for exploration-class missions with multiple iterations tested aboard the International Space Station.

6.5.3 Fundamental Research

Neutron scattering utilizes position-sensitive detectors for materials research with 2D imaging capability and high position resolution for small-angle scattering studies. Dark matter searches employ ultra-low background detection systems with cryogenic operation and sophisticated background rejection techniques.

6.6 Industrial Applications

6.6.1 Non-Destructive Testing (NDT)

Radiographic testing employs X-ray systems (50–450 kV) and gamma sources (^{60}Co, ^{192}Ir) for materials inspection with transition from film to digital sensors providing real-time imaging capabilities. Digital radiography uses real-time fluoroscopic systems for dynamic process monitoring with improved image quality and reduced exposure times.

6.6.2 Process Control and Measurement

Thickness gauging uses transmission and backscatter techniques employing beta sources (^{90}Sr, ^{85}Kr) for thin materials and gamma sources (^{137}Cs, ^{60}Co) for thicker materials, achieving plus or minus 0.1% thickness accuracy.

Level measurement employs nuclear level gauges with point detection for level switches and continuous measurement arrays for level profiling in process vessels. Composition analysis uses multi-energy gamma transmission for online analysis of ash content, moisture measurement through neutron moderation, and density profiling.

7 Safety Considerations and Regulations

7.1 Radiation Protection Principles

7.1.1 ALARA Implementation

The "As Low As Reasonably Achievable" principle, established by the NCRP in 1954, forms the foundation of modern radiation protection. ALARA implementation requires consideration of technology state, economic factors, and societal benefits while maintaining exposures below regulatory limits.

Three cardinal principles include time (minimize exposure duration through efficient work practices), distance (maximize separation from sources utilizing inverse square law relationships), and shielding (employ appropriate barriers to reduce radiation intensity).

7.1.2 Dose Limitation Framework

Current dose limits based on ICRP Publication 103 (2007) recommendations specify occupational workers at 20 mSv/year averaged over 5 years with maximum 50 mSv in any single year, general public at 1 mSv/year effective dose limit, and specific organs with individual organ dose limits (for example, 500 mSv/year to hands and feet).

7.2 Regulatory Framework

7.2.1 International Standards

The International Atomic Energy Agency (IAEA) International Basic Safety Standards for Protection Against Ionizing Radiation provide global harmonization of radiation protection requirements. The International Commission on Radiological Protection (ICRP) provides scientific basis for radiation protection through comprehensive publications addressing exposure scenarios, dose coefficients, and protection strategies.

7.2.2 National Regulations

United States regulatory structure includes NRC 10 CFR Part 20 "Standards for Protection Against Radiation", DOE 10 CFR Part 835 "Occupational Radiation Protection", OSHA 29 CFR 1910.1096 for general industry radiation protection, and FDA 21 CFR Parts 1000–1050 for electronic product radiation control.

Key requirements include dose limits, ALARA programs, personnel monitoring, equipment registration and licensing, incident reporting, and comprehensive record-keeping.

7.3 Personnel Monitoring and Dosimetry

7.3.1 Personal Dosimetry Systems

Passive dosimeters include TLD using LiF:Mg,Ti providing tissue-equivalent response with 10 microGy to 10 Gy range, OSL using Al_2O_3:C systems with re-readability and improved fade characteristics, and film badges representing historical method largely replaced by TLD and OSL technologies.

Active dosimeters include electronic personal dosimeters (EPD) with real-time display, alarm capabilities, and wireless data transmission for immediate dose assessment.

7.3.2 Area Monitoring

Fixed radiation monitoring systems provide continuous surveillance of work areas with automated alarm systems, data logging, and integration with facility safety systems.

8 Calibration and Measurement Techniques

8.1 NIST Traceability Framework

The National Institute of Standards and Technology maintains the national radiation standards through Standard Reference Materials (SRMs) covering approximately 80 radionuclides with typical uncertainties less than or equal to 2%.

8.1.1 Calibration Requirements

Energy calibration employs multi-point calibration using certified reference sources spanning the detector's energy range with linear channel-to-energy relationships verified through quality checks. Efficiency calibration determines absolute efficiency $\varepsilon = N_{\text{measured}}/N_{\text{emitted}}$ using NIST-traceable sources with proper geometric and matrix corrections. Linearity testing verifies response across activity ranges ensuring proportional response throughout the detector's dynamic range.

8.2 Quality Assurance Programs

8.2.1 QA/QC Protocols

Performance testing schedule includes daily background checks and detector response verification, weekly energy calibration verification using check sources, monthly efficiency verification and performance trending, quarterly complete performance evaluation and documentation review, and annual full system calibration with NIST-traceable sources.

Performance criteria include reproducibility within plus or minus 5% for repeated measurements, energy resolution monitoring through FWHM stability, and background trending to identify environmental changes.

8.2.2 Documentation Standards

Required records include calibration certificates, maintenance logs, training records, and measurement data with unbroken traceability chains to national standards. Retention requirements specify lifetime retention for personnel dose records, 3–5 years for equipment calibration data, and permanent retention for incident reports.

9 Data Analysis and Interpretation Methods

9.1 Statistical Analysis Fundamentals

9.1.1 Counting Statistics

Radiation detection follows Poisson distribution principles with standard deviation $\sigma = \sqrt{N}$ where N represents the number of counts. Relative uncertainty equals $1/\sqrt{N}$, emphasizing the importance of adequate counting statistics.

Confidence levels of 68% (plus or minus 1 sigma), 95% (plus or minus 2 sigma), and 99% (plus or minus 3 sigma) provide statistical confidence in measurement results.

9.1.2 Uncertainty Propagation

For combined measurements, uncertainty propagation follows addition/subtraction with

$$\sigma_{\text{total}} = \sqrt{\sigma_1^2 + \sigma_2^2 + \dots}$$

and multiplication/division with

$$\frac{\sigma_{\text{total}}}{x_{\text{total}}} = \sqrt{(\sigma_1/x_1)^2 + (\sigma_2/x_2)^2 + \dots}$$

.

9.2 Spectral Analysis Techniques

9.2.1 Peak Identification and Analysis

Spectral features include photopeak providing full energy absorption for isotope identification, Compton continuum from partial energy deposition creating background, escape peaks characteristic of pair production interactions, and backscatter peaks from 180 degree scattered radiation detection.

Analysis methods include library matching against nuclide databases, energy window analysis (plus or minus 10% photopeak ranges), and multi-peak deconvolution for overlapping peak resolution.

9.2.2 Background Subtraction Techniques

Subtraction methods include simple subtraction with $N_{\text{net}} = N_{\text{gross}} - N_{\text{background}}$, time-weighted accounting for different counting periods, region-of-interest background interpolation under peaks, and mathematical modeling using polynomial or exponential background fits.

9.3 Minimum Detectable Activity (MDA) Calculations

The standard MDA formula for 95% confidence level:

$$\text{MDA} = \frac{2.71 + 4.65\sqrt{B \times t_b}}{\varepsilon \times t_s} \tag{19}$$

where B is background counts, t_b is background counting time, t_s is sample counting time, and ε is detection efficiency.

MARSSIM implementation through the Multi-Agency Radiation Survey and Site Investigation Manual provides standardized MDA calculations for environmental remediation projects.

10 Current Research and Future Developments

10.1 Emerging Detector Materials

10.1.1 Perovskite Semiconductors

$CsPbBr_3$ represents the most significant materials breakthrough, demonstrating record energy resolutions of 2.5% at 141 keV and 1.0% at 662 keV. Recent work (Nature Communications, 2025) achieved single-photon gamma-ray imaging with solution-based processing for cost-effective manufacturing, superior stopping power compared to traditional CZT detectors, self-healing capabilities and radiation tolerance, and near-unity charge collection efficiency.

10.1.2 Wide Bandgap Semiconductors

NASA's development of silicon carbide (SiC), gallium phosphide (GaP), and zinc oxide (ZnO) detectors offers enhanced radiation tolerance for space applications and extreme environment operation.

10.2 Advanced Digital Processing

10.2.1 FPGA-Based Systems

Modern field-programmable gate array implementations enable real-time digital pulse processing with 14-bit, 125 MHz digitizers, multichannel capability supporting up to 64 detector channels, advanced algorithms including trapezoidal shaping and pile-up rejection, and sub-nanosecond timing resolution for coincidence applications.

10.2.2 Machine Learning Integration

Deep learning applications include radioisotope identification using neural networks achieving greater than 98% accuracy for 14 target radionuclides, spectral analysis using CNNs outperforming traditional methods by 2–12%, real-time processing using GPU-accelerated algorithms for high-rate detector data, and anomaly detection using ML algorithms for unusual radiation event identification.

Explainable AI (XAI) employs SHAP and LIME methodologies providing transparency in AI-driven spectral analysis decisions, enabling user confidence in automated systems.

10.3 Quantum Sensing Technologies

10.3.1 Nitrogen-Vacancy Centers

Diamond-based NV centers enable molecular-level detection sensitivity, achieving individual nuclear quadrupolar resonance signal detection at room temperature with applications in fundamental physics and materials science.

10.3.2 Superconducting Quantum Detectors

Thermal Kinetic Inductance Detectors (TKIDs) achieve tens of eV energy resolution with single-photon sensitivity for dark matter searches, kilo-pixel arrays for large-area detection, operation at sub-1K temperatures, and applications in fundamental physics and astronomy.

10.4 Future Technology Roadmap

10.4.1 Near-Term Developments (2025–2030)

Expected developments include commercial deployment of perovskite semiconductor detectors, widespread adoption of AI-enhanced spectroscopic analysis, room-temperature quantum sensors for specialized applications, and fully integrated wireless detection networks.

10.4.2 Long-Term Vision (2030–2040)

The long-term vision encompasses quantum-limited detection sensitivity across all radiation types, AI systems achieving human expert-level performance in complex spectral analysis, self-healing detector materials with decades-long operational lifetime, and ubiquitous radiation monitoring through cost-effective distributed sensors.

10.5 Research Challenges and Opportunities

Technical challenges include scalability of novel materials to commercial production volumes, long-term stability of perovskite detectors under operational conditions, integration complexity of multi-modal quantum sensing systems, and standardization of evaluation metrics for emerging technologies.

Research priorities include development of lead-free alternative detector materials, enhancement of quantum sensor multiplexing capabilities, advanced AI algorithms for real-time spectroscopic analysis, and cost reduction strategies for large-scale deployment.

Funding landscape includes federal support through DOE (16.1 billion dollars FY2024 R&D), NSF (7.5 billion dollars with quantum sensing programs), and DHS/DNDO (58 million dollars over 5 years for nuclear threat detection research).

11 Conclusions and Future Outlook

The field of radiation detection has evolved from simple electroscopes to sophisticated digital spectrometry systems incorporating quantum sensors, artificial intelligence, and advanced materials. This comprehensive treatise has examined the theoretical foundations, technological implementations, diverse applications, and future developments that define modern radiation detection capabilities.

11.1 Current State of Technology

Contemporary radiation detection systems achieve remarkable performance across multiple metrics including energy resolution less than 0.1% FWHM for high-resolution spectroscopy, detection sensitivity approaching single-particle detection limits, timing resolution at sub-nanosecond capability for coincidence measurements, spatial resolution at micrometer-scale position sensitivity, and count rate capability exceeding one million counts per second.

Digital signal processing has revolutionized detector performance through real-time algorithms, while AI integration enables automated analysis exceeding traditional methods. The transition to quantum sensing technologies promises unprecedented sensitivity improvements.

11.2 Emerging Paradigms

Several technological paradigms are reshaping the field. The materials revolution through perovskite semiconductors demonstrates superior performance compared to traditional detector materials with cost-effective solution-based manufacturing processes. AI integration enables machine learning algorithms achieving expert-level performance in spectroscopic analysis while providing explainable decision-making through advanced interpretability techniques. Quantum enhancement allows quantum sensors to approach fundamental sensitivity limits through exploitation of quantum mechanical phenomena including entanglement and squeezing. Network intelligence through distributed sensor networks with edge computing enables intelligent, autonomous radiation monitoring systems.

11.3 Application Impact

The technological advances documented in this treatise enable transformative capabilities across application domains. Medical physics benefits from enhanced imaging resolution and reduced patient doses through improved detector materials and AI-optimized protocols. Nuclear security gains automated threat detection with reduced false alarms through intelligent spectroscopic analysis and multi-modal sensor fusion. Environmental monitoring achieves real-time assessment of radiation environments through networked sensors with predictive analytics. Fundamental research benefits from quantum-limited sensitivity enabling exploration of physics beyond the Standard Model and materials science at atomic scales.

11.4 Future Vision

The next decade will likely witness commercial deployment of quantum-enhanced detection systems, AI achieving super-human performance in complex spectroscopic analysis, ubiquitous radiation monitoring through cost-effective sensor networks, and integration of detection capabilities into consumer electronic devices.

The convergence of quantum physics, artificial intelligence, advanced materials, and digital processing suggests unprecedented capabilities in radiation detection and measurement. These developments will enable new scientific discoveries, enhance public safety, and support the continued beneficial use of nuclear technologies across society.

The comprehensive knowledge base presented in this treatise provides the foundation for understanding current capabilities and participating in the continued advancement of radiation detection science and technology. As the field evolves toward quantum-enhanced, AI-driven systems, the fundamental principles and systematic approaches documented here will remain essential for practitioners, researchers, and decision-makers in the radiation detection community.

Acknowledgments

This comprehensive treatise synthesizes knowledge from numerous sources including peer-reviewed scientific literature, technical manuals, regulatory guidance documents, and contributions from leading research institutions worldwide. The author acknowledges the extensive contributions of the international radiation detection community in advancing the science and technology documented in this work.

References

[1] G. F. Knoll, *Radiation Detection and Measurement*, 4th Edition, John Wiley & Sons, Hoboken, NJ, 2010.

[2] J. E. Turner, *Atoms, Radiation, and Radiation Protection*, 3rd Edition, Wiley-VCH, Weinheim, Germany, 2007.

[3] R. D. Evans, *The Atomic Nucleus*, McGraw-Hill, New York, 1955.

[4] E. Segrè, *Nuclei and Particles*, 2nd Edition, W. A. Benjamin, Reading, MA, 1977.

[5] W. R. Leo, *Techniques for Nuclear and Particle Physics Experiments*, 2nd Edition, Springer-Verlag, Berlin, 1994.

[6] N. Tsoulfanidis and S. Landsberger, *Measurement and Detection of Radiation*, 4th Edition, CRC Press, Boca Raton, FL, 2010.

[7] C. Grupen and B. Shwartz, *Particle Detectors*, 2nd Edition, Cambridge University Press, Cambridge, UK, 2008.

[8] K. Kleinknecht, *Detectors for Particle Radiation*, 2nd Edition, Cambridge University Press, Cambridge, UK, 1998.

[9] G. Gilmore, *Practical Gamma-Ray Spectrometry*, 2nd Edition, John Wiley & Sons, Chichester, UK, 2008.

[10] International Commission on Radiological Protection, *The 2007 Recommendations of the International Commission on Radiological Protection*, ICRP Publication 103, Ann. ICRP 37 (2-4), 2007.

[11] International Atomic Energy Agency, *Radiation Protection and Safety of Radiation Sources: International Basic Safety Standards*, IAEA Safety Standards Series No. GSR Part 3, Vienna, 2014.

[12] National Council on Radiation Protection and Measurements, *Ionizing Radiation Exposure of the Population of the United States*, NCRP Report No. 160, Bethesda, MD, 2009.

[13] H. Cember and T. E. Johnson, *Introduction to Health Physics*, 4th Edition, McGraw-Hill Medical, New York, 2009.

[14] B. Shleien, L. A. Slaback Jr., and B. K. Birky, *Handbook of Health Physics and Radiological Health*, 3rd Edition, Lippincott Williams & Wilkins, Baltimore, MD, 1998.

[15] F. H. Attix, *Introduction to Radiological Physics and Radiation Dosimetry*, John Wiley & Sons, New York, 2004.

[16] E. B. Podgorsak, *Radiation Oncology Physics: A Handbook for Teachers and Students*, International Atomic Energy Agency, Vienna, 2005.

[17] H. E. Johns and J. R. Cunningham, *The Physics of Radiology*, 4th Edition, Charles C Thomas, Springfield, IL, 1983.

[18] F. M. Khan, *The Physics of Radiation Therapy*, 3rd Edition, Lippincott Williams & Wilkins, Philadelphia, PA, 2003.

[19] S. R. Cherry, J. A. Sorenson, and M. E. Phelps, *Physics in Nuclear Medicine*, 4th Edition, Elsevier Saunders, Philadelphia, PA, 2012.

[20] J. T. Bushberg, J. A. Seibert, E. M. Leidholdt Jr., and J. M. Boone, *The Essential Physics of Medical Imaging*, 3rd Edition, Lippincott Williams & Wilkins, Philadelphia, PA, 2011.

[21] W. R. Hendee and E. R. Ritenour, *Medical Imaging Physics*, 4th Edition, John Wiley & Sons, New York, 2002.

[22] S. Webb, *The Physics of Medical Imaging*, Institute of Physics Publishing, Bristol, UK, 2000.

[23] P. Sprawls, *Physical Principles of Medical Imaging*, 2nd Edition, Medical Physics Publishing, Madison, WI, 1995.

[24] Z. H. Cho, J. P. Jones, and M. Singh, *Foundations of Medical Imaging*, John Wiley & Sons, New York, 2010.

[25] M. N. Wernick and J. N. Aarsvold, *Emission Tomography: The Fundamentals of PET and SPECT*, Academic Press, San Diego, CA, 2004.

[26] F. H. Fahey, *Data Acquisition in PET Imaging*, Journal of Nuclear Medicine Technology, Vol. 30, No. 2, pp. 39-49, 2002.

[27] M. E. Phelps, *Positron Emission Tomography: Fundamentals and Clinical Applications*, Springer-Verlag, New York, 2000.

[28] D. L. Bailey, D. W. Townsend, P. E. Valk, and M. N. Maisey, *Positron Emission Tomography: Basic Sciences*, Springer-Verlag, London, 2005.

[29] J. A. Sorenson and M. E. Phelps, *Physics in Nuclear Medicine*, 2nd Edition, Grune & Stratton, Orlando, FL, 1987.

[30] H. N. Wagner Jr., Z. Szabo, and J. W. Buchanan, *Principles of Nuclear Medicine*, 2nd Edition, W. B. Saunders, Philadelphia, PA, 1995.

The End